

Central Lancashire Online Knowledge (CLoK)

Title	Precision and Accuracy of Dimensional Assessment of Luminal Contours by
	Commercially Available Quantitative Angiography Software as a
	Prerequisite to Angiography Based FFR and Other Derived Parametrics
Type	Article
URL	https://clok.uclan.ac.uk/id/eprint/55884/
DOI	https://doi.org/10.1002/ccd.31670
Date	2025
Citation	Tobe, Akihiro, Miyashita, Kotaro, Revaiah, Pruthvi C., Tsai, Tsung-Ying, Oshima, Asahi, Hu, Shiuan Hao, Sevestre, Emelyne, Garg, Scot, Bourantas, Christos et al (2025) Precision and Accuracy of Dimensional Assessment of Luminal Contours by Commercially Available Quantitative Angiography Software as a Prerequisite to Angiography Based FFR and Other Derived Parametrics. Catheterization and Cardiovascular Interventions, 106 (2). pp. 1162-1172. ISSN 1522-1946
Creators	Tobe, Akihiro, Miyashita, Kotaro, Revaiah, Pruthvi C., Tsai, Tsung-Ying, Oshima, Asahi, Hu, Shiuan Hao, Sevestre, Emelyne, Garg, Scot, Bourantas, Christos, Girasis, Chrysafios, Wentzel, Jolanda J., Onuma, Yoshinobu and Serruys, Patrick W.

It is advisable to refer to the publisher's version if you intend to cite from the work. https://doi.org/10.1002/ccd.31670

For information about Research at UCLan please go to http://www.uclan.ac.uk/research/

All outputs in CLoK are protected by Intellectual Property Rights law, including Copyright law. Copyright, IPR and Moral Rights for the works on this site are retained by the individual authors and/or other copyright owners. Terms and conditions for use of this material are defined in the http://clok.uclan.ac.uk/policies/



Central Lancashire Online Knowledge (CLoK)

Title	Precision and Accuracy of Dimensional Assessment of Luminal Contours by Commercially Available Quantitative Angiography Software as a Prerequisite to Angiography Based FFR and Other Derived Parametrics
Туре	Article
URL	https://clok.uclan.ac.uk/id/eprint/55884/
DOI	https://doi.org/10.1002/ccd.31670
Date	2025
Citation	Tobe, Akihiro, Miyashita, Kotaro, Revaiah, Pruthvi C., Tsai, Tsung-Ying, Oshima, Asahi, Hu, Shiuan Hao, Sevestre, Emelyne, Garg, Scot, Bourantas, Christos et al (2025) Precision and Accuracy of Dimensional Assessment of Luminal Contours by Commercially Available Quantitative Angiography Software as a Prerequisite to Angiography Based FFR and Other Derived Parametrics. Catheterization and Cardiovascular Interventions. ISSN 1522-726X
Creators	Tobe, Akihiro, Miyashita, Kotaro, Revaiah, Pruthvi C., Tsai, Tsung-Ying, Oshima, Asahi, Hu, Shiuan Hao, Sevestre, Emelyne, Garg, Scot, Bourantas, Christos, Girasis, Chrysafios, Wentzel, Jolanda J., Onuma, Yoshinobu and Serruys, Patrick W.

It is advisable to refer to the publisher's version if you intend to cite from the work. https://doi.org/10.1002/ccd.31670

For information about Research at UCLan please go to http://www.uclan.ac.uk/research/

All outputs in CLoK are protected by Intellectual Property Rights law, including Copyright law. Copyright, IPR and Moral Rights for the works on this site are retained by the individual authors and/or other copyright owners. Terms and conditions for use of this material are defined in the http://clok.uclan.ac.uk/policies/



ORIGINAL ARTICLE - CLINICAL SCIENCE OPEN ACCESS

Precision and Accuracy of Dimensional Assessment of Luminal Contours by Commercially Available Quantitative Angiography Software as a Prerequisite to Angiography Based FFR and Other Derived Parametrics

Akihiro Tobe¹ | Kotaro Miyashita¹ | Pruthvi C. Revaiah¹ | Tsung-Ying Tsai¹ | Asahi Oshima¹ | Shiuan Hao Hu¹ | Emelyne Sevestre¹ | Scot Garg²³¹ | Christos Bourantas⁴⁵¹ | Chrysafios Girasis⁶ | Jolanda J. Wentzel⁵ | Yoshinobu Onuma¹ | Patrick W. Serruys¹

¹CORRIB Research Centre for Advanced Imaging and Core Laboratory, University of Galway, Galway, Ireland | ²Department of Cardiology, Royal Blackburn Hospital, Blackburn, UK | ³School of Medicine, University of Central Lancashire, Preston, UK | ⁴Department of Cardiology, Barts Heart Center, Barts Health NHS Trust, London, UK | ⁵Cardiovascular Devices Hub, Centre for Cardiovascular Medicine and Devices, William Harvey Research Institute, Queen Mary University of London, London, UK | ⁶EUROMEDICA General Clinic of Thessaloniki, Thessaloniki, Greece | ⁷Department of Cardiology, Erasmus Medical Center, Rotterdam, The Netherlands

Correspondence: Patrick W. Serruys (patrick.w.j.c.serruys@gmail.com)

Received: 31 January 2025 | Revised: 25 May 2025 | Accepted: 29 May 2025

Funding: The authors received no specific funding for this work.

ABSTRACT

Background: Accurate dimensional measurements are critical for quantitative coronary angiography (QCA) and serve as the first step in angiography-based fractional flow reserve (FFR) calculations.

Aims: To compare minimum lumen diameter (MLD) measurements across multiple QCA or anigo-based FFR software programs using phantom models.

Methods: Fourteen QCA and angio-based FFR programs were evaluated using six plexiglass phantoms, each containing three sequential bifurcations with known true values for the MLD of the proximal main, distal main, and side branch vessels. The accuracy and precision of MLD measurements were assessed by comparing software-measured values with true values across 54 MLD measurement points. No manual correction of the vessel contour was performed. The results of the 14 programs were reported anonymously.

Results: The mean differences between the measured and true values were small (< 0.1 mm), however, in two angio-based FFR programs, the discrepancies were large (> 0.3 mm). The standard deviations of the differences were approximately 0.1 mm, except in one angio-based FFR program, where it exceeded 0.3 mm. Differences from true values were more pronounced in small ($\le 0.7 \text{ mm}$) compared to large (> 0.7 mm) true MLDs. The reproducibility of measurements was high (Pearson's correlation coefficient > 0.98) across all programs.

Conclusion: Variations in MLD measurements were observed among different QCA and angio-based FFR programs. These variations may influence diagnostic performance and can seriously impact decisions made solely using angio-based FFR.

This is an open access article under the terms of the Creative Commons Attribution-NonCommercial License, which permits use, distribution and reproduction in any medium, provided the original work is properly cited and is not used for commercial purposes.

© 2025 The Author(s). Catheterization and Cardiovascular Interventions published by Wiley Periodicals LLC.

1 | Introduction

Quantitative coronary angiography (QCA) provides an accurate and objective assessment of the luminal dimensions of coronary artery disease (CAD) [1]. In the early eighties, only twodimensional (2D) single vessel QCA assessments applied to a single angiographic projection were available. The development of an algorithm for the accurate and precise assessment of contour detection was an intricate process, which first required a search for the optimal threshold for edge contour detection between the first and second derivatives of the brightness function. The final choice for the algorithm, which was designed more than 40 years ago, but has stood the test of time, was to use the weighted average of the two derivatives. In 1995, Keane et al. anonymously compared the accuracy and precision in luminal dimensions of 10 QCA software packages and confirmed marked variability in performance; only two of them have passed the test of time [2].

From the advent of QCA imaging technology, it was obvious that there was a gap between the simple morphological assessment of stenoses and their complex functional impact [3]. This led to the emergence of invasive fractional flow reserve (FFR), which could estimate the functional severity of a stenosis and optimize decision-making for a functionally "justified" revascularization. The effectiveness of FFR is widely validated and broadly used in clinical practice [4–6]. Its drawback, however, is the invasiveness of inserting a pressure wire into the coronary artery and the need for the induction of maximal hyperemia, which frequently causes patients discomfort.

Angiography-based FFR is a surrogate technology built upon the principles of QCA, providing virtual pullbacks of FFR without needing a pressure wire pullback during continuous hyperemia. It is computed from fluid dynamic principles and the reconstruction of a 3D model of the coronary artery [7–10]. For angiography-based FFR, accurate and precise measurements of vessel dimensions are essential since computational fluid dynamics use classical hemodynamic equations, such as the Lance-Gould and the Navier—Stokes equations, and require assessment of the entry and exit angle, length of the obstruction, and measurement of the minimal area [1, 11]. It follows that if the dimensional measurements are not accurate, the derived angio-based FFR would also not be accurate.

Therefore, the aim of the current study is to compare and validate the accuracy and precision of measuring vessel dimensions among different QCA and QFR software programs using phantom models. This study anonymously investigated one of the basic measurements of QCA, the minimal lumen diameter (MLD), in coronary phantoms with serial side branches (SB) of known dimensions using 14 different QCA and angio-based FFR software programs.

2 | Methods

2.1 | Phantoms

Six plexiglass phantoms were created, and their manufacturing details are described elsewhere [12]. In brief, the phantoms were created for the validation of bifurcation QCA software. Each phantom has three successive bifurcations, with each bifurcation having at least one stenosis, and the MLD located within 3–6 mm from the point of bifurcation (Figure 1). The Medina classification, reference vessel diameter, MLD, lesion length and shape, and angulation of each bifurcation were designed based on relevant literature. The phantoms were manufactured with a tolerance of < 10 μm from the 3D luminal surface description exported in Surface Tesselation Language (STL) file format. The true MLD was determined from the 3D luminal surface description using VMTK (Vascular Modeling Toolkit v0.7). The bifurcations of the phantoms were created in the same plane, and all lesions were made circular.

The MLDs of the proximal main branch (PMV), distal main branch (DMV), and SB within 6 mm from each bifurcation point were measured: in total, 54 MLDs were measured in each software program. There were 33 stenoses within 3–6 mm of the bifurcation point (MLD ranging from 0.53 to 1.96 mm), whereas there were 21 non-stenoses ranging from 1.40 to 4.00 mm.

2.2 | Acquisition and Calibration

The digital angiograms were acquired on a biplane angiographic system (Axiom Artis, Siemens, Forchheim, Germany). All phantoms were filled with 100% Iodixanol 320 (Visipaque, GE Healthcare, Cork, Ireland) and imaged at 30 frames per second, in a 20 cm field, with the center of the phantom placed precisely at the isocenter. For 2D QCA and 2D angio-

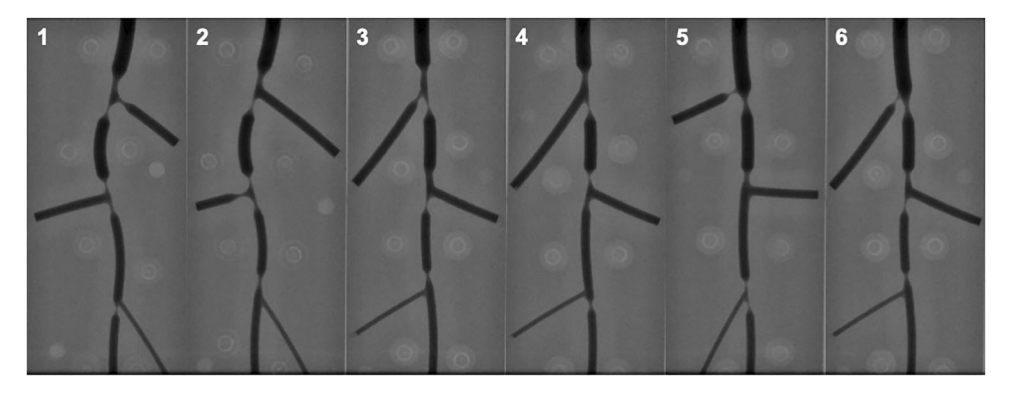


FIGURE 1 | Six plexiglass phantoms (AP views).

based FFR analyses, images were acquired in the anteroposterior (AP) direction. For 3D QCA and 3D angio-based FFR analyses, images were acquired in right- and left-anterior oblique 30° with cranial/caudal 0° (RAO30° and LAO30°).

For the QCA and angio-based FFR analyses based on 2D images, pixel calibration was performed on a 10 mm grid board acquired in the AP direction, with the recording geometry of the X-ray system obtained from the DICOM (Digital Imaging and

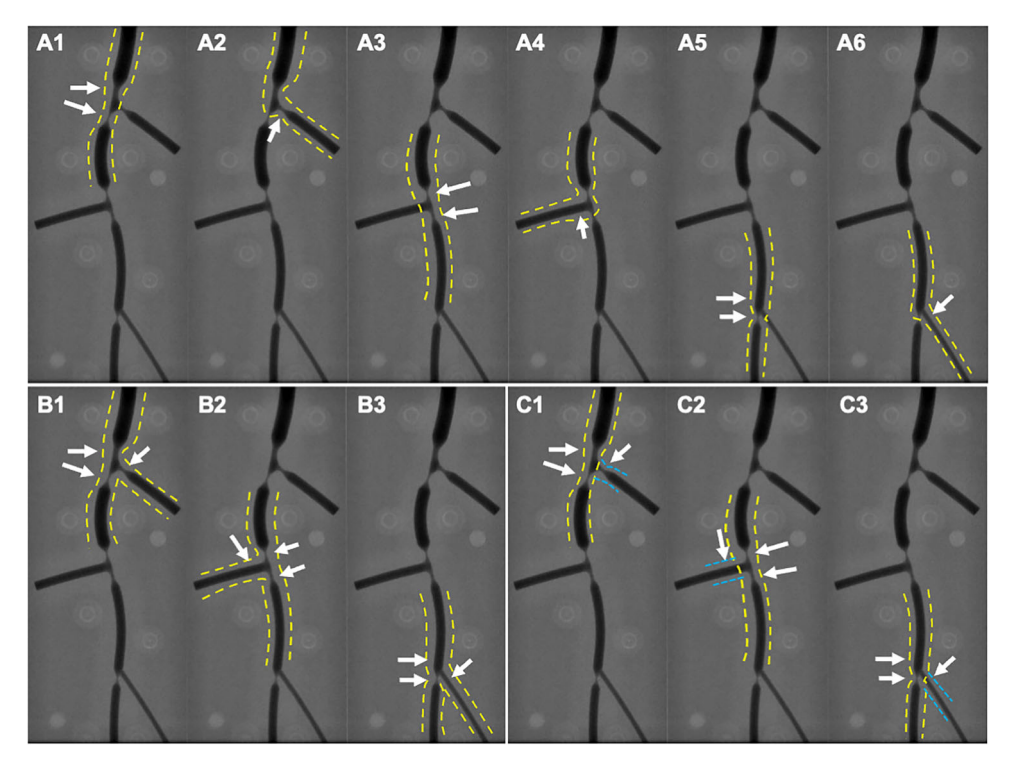


FIGURE 2 | Analysis segment 1: Per bifurcation analysis. (A) MV analysis (PMV to DMV) of the first bifurcation (A1), second bifurcation (A3), and third bifurcation (A5). SB analysis (PMV to SB) of the first bifurcation (A2), second bifurcation (A4), and third bifurcation (A6). (B) Analysis with bifurcation QCA software of the first bifurcation (B1), second bifurcation (B2), and third bifurcation (B3). (C) In two software programs, the measurement of SB was automatically derived from the main branch analysis (C1–C3). The white arrow indicates the measurement point of MLD. The yellow dotted line indicates the analysis segment. The blue dotted line indicates the analysis segment of the SB automatically derived from the main branch analysis. DMV = distal main vessel, MLD = minimal lumen diameter, MV = main vessel, PMV = proximal main vessel, QCA = quantitative coronary angiography, SB = side branch. [Color figure can be viewed at wileyonlinelibrary.com]

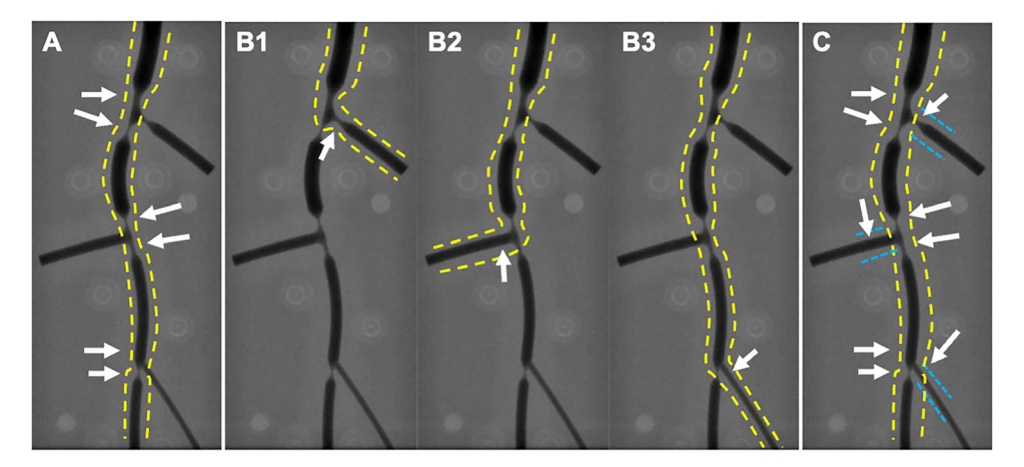


FIGURE 3 | Analysis segment 2: Total segment analysis. (A) MV analysis (from the most proximal to the most distal point of MV). The six MLDs (first PMV and DMV, second sequential PMV and DMV, and third sequential PMV and DMV) were measured. (B) SB analysis (from the most proximal point of the MV to the most distal point of the target SB). The MLDs of the first SB (B1), second SB (B2), and third SB (B3) were measured. (C) In two software programs which provide the measurements of the side branches automatically from the main branch analysis, the automatic measurements were used as the MLDs of the side branches. The white arrow indicates the measurement point. The yellow dotted line indicates the analysis segment. The blue dotted line indicates the analysis segment of the side branch automatically derived from the main branch analysis. DMV = distal main vessel, MLD = minimal lumen diameter, MV = main vessel, PMV = proximal main vessel, SB = side branch. [Color figure can be viewed at wileyonlinelibrary.com]

TABLE 1 | The mean \pm SD values of the true and software-measured MLDs.

Metric	Per bifurcation analysis Mean ± SD (mm)	Total segment analysis Mean ± SD (mm)
True MLD	1.48 ± 0.84	1.48 ± 0.84
2D single vessel QCA		
A	1.51 ± 0.81	1.51 ± 0.82
В	1.51 ± 0.79	1.52 ± 0.79
2D bifurcation QCA		
C	1.55 ± 0.80	_
D	1.51 ± 0.77	_
E	1.50 ± 0.76	_
2D angio-based FFR		
F	1.53 ± 0.73	1.54 ± 0.73
3D single vessel QCA		
G	1.48 ± 0.80	1.49 ± 0.80
Н	1.51 ± 0.78	1.51 ± 0.78
3D bifurcation QCA		
I	1.50 ± 0.81	_
J	1.57 ± 0.76	_
3D angio-based FFR		
K	1.55 ± 0.78	1.55 ± 0.78
L	1.51 ± 0.79	1.51 ± 0.78
M	1.81 ± 0.82	1.81 ± 0.82
N	1.86 ± 0.88	1.90 ± 0.92

Note: Measurements in all (n = 54) measurement points.

Abbreviations: FFR = fractional flow reserve, QCA = quantitative coronary angiography, SD = standard deviation.

Communications in Medicine) header, and the phantom's thickness taken into account to determine the true pixel size in the phantom plane [12]. Radiographic system settings, phantom arrangement, table height, and source to image intensifier distance were kept constant throughout each phantom-cm grid acquisition and were identical for all phantoms.

For the QCA and angio-based FFR analyses based on 3D reconstruction, voxel calibration was performed by each software's algorithm in the RAO30° and LAO30° projections.

2.3 | QCA and Angiography-Based FFR Software

In total, 14 different QCA and angio-based FFR software programs were validated; nine QCA programs including two 2D single vessel (CAAS Workstation 8.2.4 2D [PieMedical, Maastricht, The Netherlands], QAngio XA 8.0 2D [Medis, Leiden, The Netherlands]), two 3D single vessel (CAAS Workstation 8.2.4 3D, QAngio XA 3D 2.2 3D), three 2D bifurcation (CAAS Workstation 8.2.4 2D bifurcation, 2D bifurcation BSM-11, 2D bifurcation BSM-6), and two 3D bifurcation programs (CAAS Workstation 8.2.4 3D bifurcation and QAngio XA 3D 2.2 3D bifurcation); and five angio-based FFR programs including one 2D single vessel (AngioPlus 3.3.0.0 μ QFR 2D [Pulse Medical, Shanghai,

China]) and four 3D single vessel programs (AngioPlus 3.3.0.0 μ QFR 3D, CAAS Workstation 8.5.1 vFFR, QAngio XA 3D 2.2 QFR, FlashAngio system 1.0.12.13 [Rainmed Ltd., Suzhou, China]). The names of software programs were anonymized and referred to as A–N.

2.4 | QCA and Angio-Based FFR Analysis

Each QCA and angio-based FFR software analysis was performed according to the following common rules:

- The AP view was used for 2D QCA/angio-based FFR analysis, whilst the RAO 30° and LAO 30° (cranial/caudal 0°) views were used for 3D QCA/angio-based FFR analysis.
- 2. Analysis was performed using the middle frame of every angiographic image acquisition to avoid frame selection bias.
- For 2D analyses (AP view), the calculated pixel size was manually entered. For 3D analyses (RAO30 and LAO30 views), voxel calibration was performed using each software's algorithm.
- 4. Neither manual correction of vessel contour nor the use of any adjustment function of vessel contour were allowed.

 TABLE 2
 The accuracy and precision of software-measured MLDs.

		Per bifurcation	Per bifurcation analysis (mm)			Total segment	Total segment analysis (mm)	
Software-measured MLD minus true MLD	Accuracy (mean difference)	Precision (SD)	Agreement (1.96*SD)	Mean absolute difference	Accuracy (mean difference)	Precision (SD)	Agreement (1.96*SD)	Mean absolute difference
2D single vessel QCA								
А	0.022	0.071	0.139	0.064	0.026	0.062	0.121	0.057
В	0.027	0.086	0.168	0.071	0.032	0.096	0.188	0.082
2D bifurcation QCA								
C	0.070	0.139	0.273	0.116	I	I		I
D	0.023	0.108	0.212	0.086	I	I		I
ш	0.012	0.123	0.241	0.093	I	I		I
2D angio-based FFR								
ĽΊ	0.050	0.173	0.339	0.148	0.059	0.173	0.339	0.148
3D single vessel QCA								
ß	-0.001	0.076	0.150	0.065	0.008	0.080	0.157	0.070
Н	0.027	0.112	0.219	0.094	0.029	0.105	0.205	0.089
3D bifurcation QCA								
Ι	0.011	0.080	0.157	0.063	I	1		I
ſ	0.086	0.163	0.319	0.132	I	1		I
3D angio-based FFR								
K	0.064	0.101	0.198	0.099	0.062	0.104	0.203	0.102
T	0.031	0.110	0.216	0.095	0.027	0.103	0.203	0.087
M	0.324	0.139	0.273	0.324	0.325	0.162	0.317	0.325
Z	0.373	0.359	0.704	0.378	0.419	0.456	0.893	0.420

Note: Measurements in all (n = 54) measurement points. Abbreviations: FFR = fractional flow reserve, QCA = quantitative coronary angiography, SD = standard deviation.

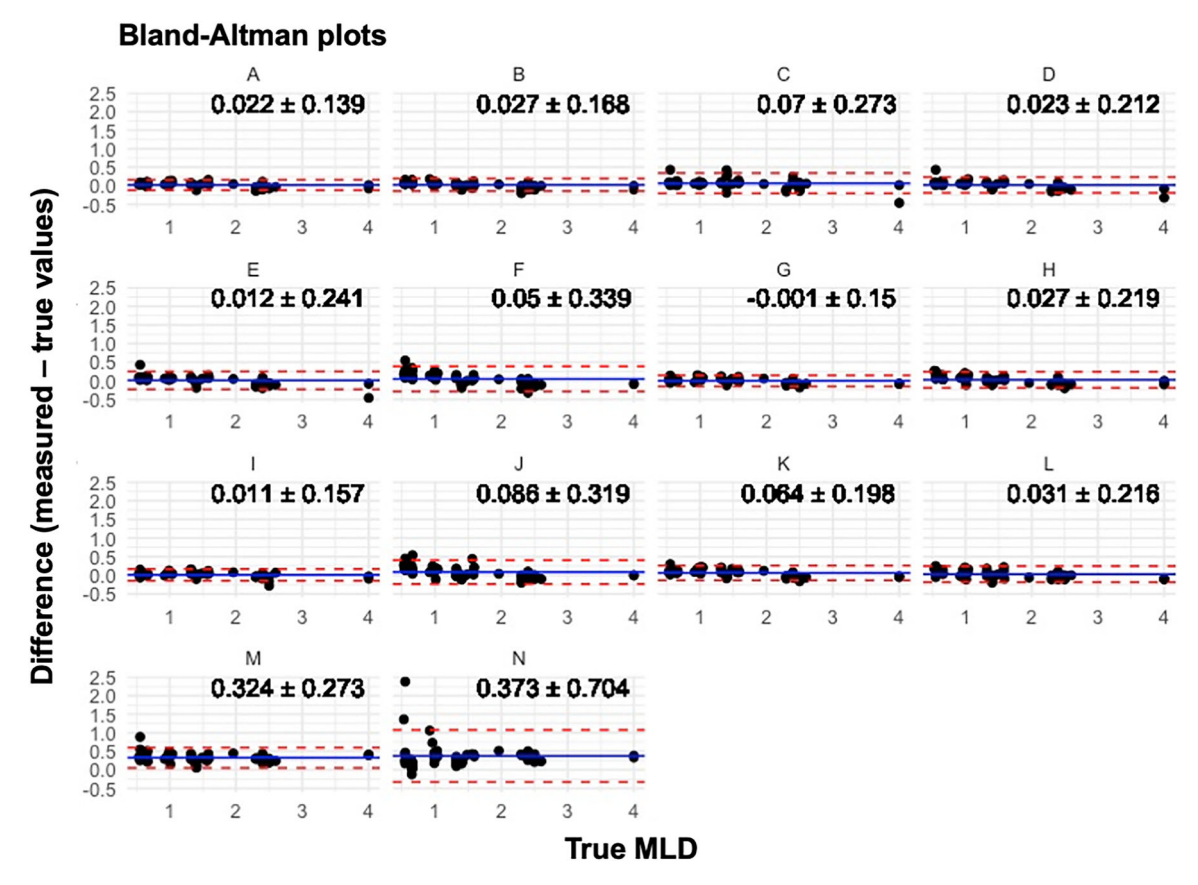


FIGURE 4 | Bland—Altman plots. The *X*-axis represents the true value, and the *Y*-axis represents the measured value minus true value. The blue line indicates the mean of the measured minus true value, and the red dotted lines represent the mean ± 1.96 SD. The numbers in the top-right corners show the mean ± 1.96 SD in each program. [Color figure can be viewed at wileyonlinelibrary.com]

- 5. For 3D analysis, the analyst was allowed to adjust the 3D corresponding point in two angiographic views.
- For angio-based FFR analysis, the automatically defined flow velocity was used if available; if not, arbitrary values (e.g., 18.4 cm/s) were substituted (this process does not affect MLD measurement).

2.5 | Analysis Segment

The QCA and angio-based FFR software were validated against calibrated phantoms using two different modes of analysis segmentation.

Analysis segmentation 1: Per bifurcation analysis (Figure 2). The proximal and distal delimiter points were placed at the furthest possible distance from the bifurcation to be analyzed, without involving the sequential bifurcation lesions or the phantom borders.

To obtain the MLDs in PMV, DMV, and SB separately, two analyses were performed per bifurcation.

- 1. MV analysis; PMV to DMV (Figure 2 A1, A3, and A5) and
- 2. SB analysis; PMV to SB (Figure 2 A2, A4, and A6).

With bifurcation QCA software, the analysis was performed simultaneously on PMV, DMV, and SB in each bifurcation (Figure 2 B1, B2, and B3). In two software programs, analyzing the main branch automatically triggered an analysis of the SB. In such cases, the MLD of the SB was derived from the main branch analysis (Figure 2 C1, C2, and C3).

Analysis segmentation 2: Total segment analysis (Figure 3). This segment analysis simulates the actual angio-based FFR analysis in clinical practice. The proximal delimiter point was always placed at the most proximal possible position of the main branch. For the analysis of the main branch, the distal delimiter point was placed at the most distal possible position of the main branch. The six MLDs in the main branch (first PMV and DMV, second sequential PMV and DMV, and third sequential PMV and DMV) were measured (Figure 3A). For the analysis of the SB, the distal delimiter point was placed at the most distal possible position of the target SB. The MLD of the target SB was measured (Figure 3 B1-B3). In two software programs which provide the MLDs of the SB automatically from the main branch analysis, such values were used as the MLDs of the SB (Figure 3C). This total segment analysis was not available in the bifurcation QCA software.

2.6 | Statistics

Statistical analysis was performed using R version 4.4.0 (SAS Institute, Cary, NC). Continuous variables are presented as mean \pm standard deviation (SD). Paired values between the true

TABLE 3 | Per bifurcation analysis in large (>0.7 mm) and small (≦0.7 mm) true MLDs.

Software-		Large ML	Large MLDs > 0.7 mm			Small MLI	Small MLDs ≦0.7 mm		Large versus small comparison (difference) ^a	Large versus small comparison (absolute difference) ^b
measured MLD minus true MLD	Accuracy (mean difference)	Precision (SD)	Agreement (1.96*SD)	Mean absolute difference	Accuracy (mean difference)	Precision (SD)	Agreement (1.96*SD)	Mean absolute difference	p value	p value
2D single vessel QCA										
А	0.010	0.076	0.150	0.065	0.057	0.037	0.073	090.0	0.03	0.97
В	0.001	0.081	0.158	090.0	0.100	0.049	0.097	0.100	< 0.01	0.03
2D bifurcation QCA										
C	0.061	0.150	0.294	0.123	0.096	0.102	0.201	960.0	0.59	0.31
D	-0.002	0.099	0.195	0.082	0.096	0.102	0.201	0.096	< 0.01	0.85
Щ	-0.017	0.117	0.229	0.091	960.0	0.102	0.201	0.096	< 0.01	0.94
2D angio- based FFR										
Ц	-0.013	0.139	0.273	0.120	0.231	0.128	0.252	0.231	< 0.01	< 0.01
3D single vessel QCA										
Ŋ	-0.007	0.084	0.165	0.075	0.016	0.046	0.090	0.034	0.34	< 0.01
Н	-0.009	0.098	0.191	0.082	0.129	0.084	0.165	0.129	< 0.01	0.08
3D bifurcation QCA										
I	0.008	0.089	0.175	0.072	0.021	0.046	0.090	0.034	0.94	< 0.01
ſ	0.029	0.125	0.246	0.091	0.250	0.148	0.290	0.250	< 0.01	< 0.01
3D angio- based FFR										
M	0.046	0.106	0.207	0.093	0.116	0.065	0.127	0.116	0.048	0.21
Г	0.001	0.106	0.207	0.086	0.114	0.076	0.149	0.121	< 0.01	0.07
										(Continues)

TABLE 3 | (Continued)

Large versus small small comparison comparison (absolute (difference) ^a difference) ^b		difference p value p value	0.409 0.03 0.03	0.439 0.07 0.08
s ≦ 0.7 mm	Me Agreement abso		0.337 0.4	1.301 0.4
Small MLDs ≦0.7 mm	Precision	(SD)	0.172	0.664
	Accuracy (mean	difference)	0.409	0.421
	Mean absolute	difference	0.295	0.357
Large MLDs > 0.7 mm	Agreement	(1.96*SD)	0.223	0.324
Large MLI	Precision	(SD)	0.114	0.166
	Accuracy (mean	difference)	0.295	0.357
Software-	measured MLD minus	true MLD	M	Z

The absolute differences between measured and true values were compared between large and small vessels. p values were calculated using the Mann-Whitney U test 'The differences between measured and true values were compared between large and small vessels. p values were calculated using the Mann-Whitney U test. true MLDs (≦ 0.7 mm) are tabulated. in the large true MLDs (> 0.7 mm) and in the small Note: The results

MLD and software-measured MLD were compared using a paired t-test. The individual signed differences (software-measured MLD minus true MLD) were averaged; the mean of these signed differences is a measure of accuracy (i.e., systematic error); the standard deviation is a measure of precision (i.e., random error). The mean absolute difference (MAD) was defined as the mean of I signed difference I. Additionally, the signed differences were compared between the large true MLD group (> 0.7 mm) and the small true MLD group (≤0.7 mm). The agreement in MLD between the true and software-measured MLD was evaluated using the Bland-Altman plot. The reproducibility was evaluated using two methods: the first assessed the intra-observer reproducibility of the per-bifurcation analysis in each software performed with a time interval of greater than 30 days. The second method evaluated the reproducibility between per-bifurcation analysis and total segment analysis for each software. The mean and SD of signed differences between the two analyses were calculated; the repeatability coefficient was calculated as 1.96 times the SD, indicating that 95% of the repeated measurements fall within this range. The Pearson's correlation coefficient was calculated to examine the relationship between the two reproducibility measurements. All statistical tests were two-sided and a p < 0.05 was considered statistically significant.

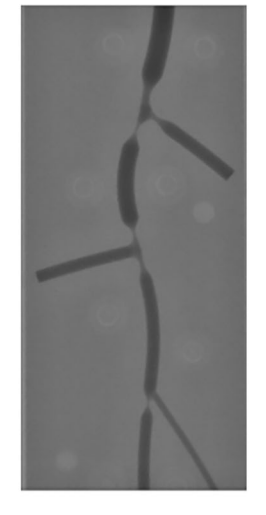
3 | Results

The mean + SD values of the true and software-measured MLDs in 54 measurement points are listed in the Table 1. The mean value of the true MLDs was 1.48 ± 0.84 mm. The accuracy (mean difference) and precision (SD) of each software compared with the true MLDs are summarized in Table 2 and the Bland-Altman plots are displayed in Figure 4. In the per bifurcation analysis, software programs A, G, and I had favorable accuracy and precision (A: 0.022 ± 0.071 mm, G: -0.001 ± 0.076 mm, I: 0.011 ± 0.080 mm). The mean differences between software-measured and true values were < 0.1 mm in 12 programs; however, in two programs (M and N), the discrepancies were $> 0.3 \,\mathrm{mm}$ (M: $0.324 \pm 0.139 \,\mathrm{mm}$, N: 0.373 ± 0.359 mm). The standard deviations of the differences between measured and true values were approximately 0.1 mm in 13 programs, whereas in software program N, it was greater than 0.3 mm. The result of total segment analysis was similar with that of the per-bifurcation analysis.

The intra-observer reproducibility in the per bifurcation analysis and the reproducibility between the per bifurcation versus total segment analysis, are shown in the Supporting Information S1: Tables 1 and 2. The intra-observer reproducibility of measurements was high for each software (Pearson's correlation coefficient > 0.98). The reproducibility between the per bifurcation and total segment analysis in the program N was relatively low (0.93) compared to other programs (> 0.99).

The results in the large (> 0.7 mm) and small (\leq 0.7 mm) true MLDs are tabulated in Table 3. In phantoms with small MLDs, the mean difference between true MLD and software-measured MLD was greater than in phantoms with large MLDs except for software C, G, I, and N. For example, in large MLD phantoms, software B accurately measured MLD with a mean difference of 0.001 mm, whereas in small MLD phantoms, software B overestimated MLD by 0.100 mm.

MLD measurement was performed with 14 QCA and angio-based FFR programs (A-N) in six phantoms with known MLD

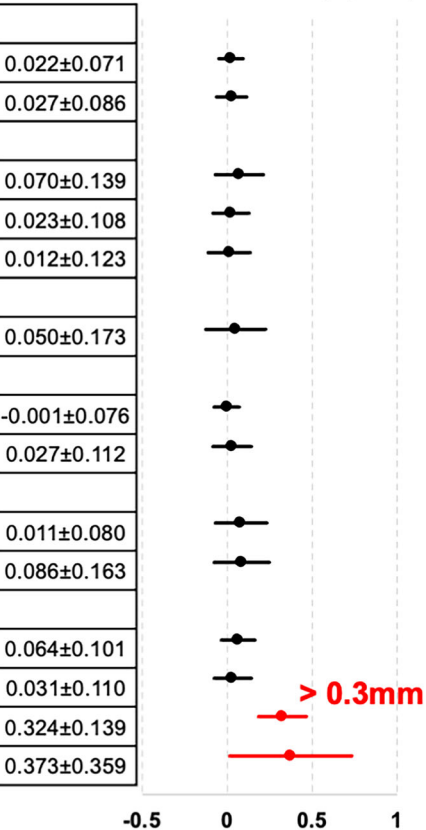


values.



2D single vessel QCA	
А	0.022±0.071
В	0.027±0.086
2D bifurcation QCA	
С	0.070±0.139
D	0.023±0.108
E	0.012±0.123
2D angio-based FFR	
F	0.050±0.173
3D single vessel QCA	
G	-0.001±0.076
Н	0.027±0.112
3D bifurcation QCA	
1	0.011±0.080
J	0.086±0.163
3D angio-based FFR	
К	0.064±0.101
L	0.031±0.110
М	0.324±0.139

Difference (Measured minus true value) (mm)



Simulated impact of a -0.3mm difference in MLD measurement on angio-based FFR

Lance Gould's equation			adjustment MLD		ced adjustment D by -0.3 mm
	Pulse 2D		MLD=1.2 mm μ QFR =0.90		MLD=0.9mm μ QFR =0.78
F: coefficient of friction S: coefficient of separation µ: viscosity L: stenosis length An: normal cross-sectional area	Pulse 3D		MLD=1.3 mm μ QFR =0.86		MLD=1.0 mm μ QFR =0.75
As: stenotic cross-sectional a V: flow velocity	rea Medis	O'R CE	MLD=1.3 mm QFR=0.89		MLD=1.0 mm QFR=0.79
A Frank	RainMed		MLD=1.4 mm caFFR=0.83		MLD=1.1 mm caFFR=0.74
	PieMedica		MLD=1.2 mm vFFR=0.87	, o	MLD=0.9 mm vFFR=0.77

CENTRAL ILLUSTRATION 1 | Legend on next page.

4 | Discussion

The MLD measurements of 14 different QCA/angio-based FFR software programs were validated using bifurcation phantoms for which the true MLDs were known. The mean differences between software-measured and true values (i.e., accuracy or systematic error) were generally small (< 0.1 mm), whereas in two software programs (M and N) these discrepancies were large (> 0.3 mm). The standard deviations of the differences between software-measured and true values (i.e., precision or random error) were around 0.1 mm, whereas in software program N, it was more than 0.3 mm. The reproducibility of measurements was high (Pearson's correlation coefficient greater than 0.98) for each software.

Accurate dimensional measurements are essential for QCA and the first basic requirement in calculating an accurate angio-based FFR, which relies on a 3D vessel reconstruction, and is then computed using software-specific fluid dynamic algorithms (such as Lance-Gould's or Navier-Stokes equations). Inaccurate dimensions lead to inaccuracies and a lack of reliability in derived parameters, which is not limited to just the angio-based FFR, but includes the pressure pullback gradient index (PPGi), instantaneous angiobased FFR gradient per unit (dangio-based FFR/ds), and the index of microcirculation resistance (IMR). For example, as shown in Table 2, two software programs had a discrepancy in MLD from the true value of ≥ 0.3 mm. To simulate the potential impact of this difference on clinical decisions, angio-based FFR assessment with and without forced adjustment of the MLD was performed in a left anterior descending artery with an intermediate stenosis (Central Illustration 1). The measured MLD ranged from 1.2 to 1.4 mm with angio-based FFR values of 0.83 to 0.90. Despite this variability, all angio-based FFR values were interpreted as physiologically negative (> 0.80), and the lesion would be deferred. Assuming that the software overestimates MLD by 0.3 mm, MLD was forcefully corrected by -0.3 mm. This subtle change in MLD reduced the angiobased FFR values by 0.09 to 0.12, resulting in a range of 0.74 to 0.79. These adjusted values would now be interpreted as physiologically positive (≤ 0.80), indicating the need for revascularization. Hence, when using angiography-based physiological assessment, an overestimation of MLD by as little as 0.3 mm could change a clinical decision for and against revascularization.

To ensure the reproducibility of our analysis, manual correction of vessel contours was not permitted. Vessel contour delineation with software program N was sometimes significantly offset from the phantom's edge, resulting in a large discrepancy from the true value. In software program M, vessel contour delineation was not an issue, but there was still a large discrepancy from the true value. To ensure the accuracy of our analysis, we asked the vendors of software programs M and N to conduct their own analysis, and this confirmed that these two programs had the worst performance, in keeping with our findings.

In our study, differences between software-measured and true values were larger in phantoms with relatively small true MLDs (≦0.7 mm) compared to phantoms with large true MLDs (> 0.7 mm), with a tendency for software-measured values to be overestimated compared to true values in those with small MLDs. In four out of five angio-based FFR software programs, the variance of measured diameters from the true dimensions was greater in the small compared to the large MLD group (Table 3). Current results are in line with previous studies reporting that QCA systems tend to overestimate MLD values in phantoms with small MLDs [13]. Angio-based FFR, which is built upon QCA technology, shares this limitation which potentially contributes to false negatives in cases with small MLDs. In a study by Ninomiya et al. comparing binominal diagnostic accuracies of various angio-based FFR systems against wire-based FFR, MLD was one of the contributing factors of discordance between the two. A smaller MLD was associated with an increased risk of a false-negative angiobased FFR (> 0.80) [14].

The clinical efficacy of angio-based FFR is currently being intensively investigated. The FAVOR III China trial demonstrated the clinical benefit of QFR-guided PCI over angio-guided PCI in terms of the composite endpoint of all-cause mortality, myocardial infarction or ischemia-driven revascularization at 1 year (5.8% vs. 8.8%, p = 0.0004) and 2 years (8.5% vs. 12.5%, p < 0.0001) [7]. Deferral of revascularization based on QFR was related with a higher incidence of adverse events at 1 year compared with wire FFR-based deferral [10]. On the contrary, the FAVOR III Europe trial revealed the unfavorable clinical outcomes of QFR guidance compared to wire-FFR guidance with the primary composite endpoint of death, myocardial infarction, and unplanned revascularisation occurring in 6.7% of the QFR group and in 4.2% of the wire-FFR group (hazard ratio = 1.63, p = 0.013) [9]. The ongoing PIONEER IV (QFR), FAST III (vFFR), ALL-RISE (FFRangio), and FLASH II (caFFR) trials will provide new insights into the clinical efficacy of various angio-based FFR software programs [15, 16]. Notably variations in MLD measurements amongst the angio-based FFR software, as observed in this fantom study, may contribute to heterogeneous results amongst these clinical outcome studies investigating angio-based FFR.

4.1 | Limitations

This study has several limitations. First, the phantom is a static object and does not account for the movement of actual vessels. Its surface has a smooth luminal structure, differing from real vessels with atherosclerosis. Second, the used projections were different between 2D and 3D programs: for 2D programs, AP projections of the phantoms were used for analysis, and for 3D programs, RAO30 °(CRA 0°) and LAO30 °(CRA 0°) projections were used. The bifurcations of the phantoms were created in the same plane, and all lesions were made circular. This

CENTRAL ILLUSTRATION 1 | Upper part: The mean differences between software-measured minus true values. Two software programs had a discrepancy in MLD by ≥ 0.3 mm from the true value. Lower part: Angio-based FFR assessment with and without forced adjustment of MLD was performed in a left anterior descending artery with an intermediate stenosis to simulate the potential impact of a −0.3 mm difference of MLD measurement. In all five angio-based FFR programs, angio-based FFR values were negative (> 0.80) without adjustment of MLD while they were positive (≤ 0.80) after forced adjustment of MLD. The order of software program names shown in the figure differs from the alphabetical labels used in the anonymized. [Color figure can be viewed at wileyonlinelibrary.com]

structure likely favored analysis using the 2D systems with an AP view. Third, to maintain the reproducibility of the analyses, manual corrections of vessel contours were prohibited; however, this may not fully reflect actual clinical practice.

5 | Conclusion

This phantom study demonstrated variations in MLD measurements among different QCA/angio-based FFR software programs. These variations may result in differential diagnostic performance and potentially diverse clinical outcomes with angio-based FFR depending on the type of software program.

Acknowledgments

We appreciate the intellectual support of Prof. Hans Reiber and Jean-Paul Aben and would also like to acknowledge the technical support of Pengcheng Sun and Zhen Qi.

Conflicts of Interest

Kotaro Miyashita reports a research grant from OrbusNeich Medical K.K., outside the submitted work. Scot Garg reports consulting fees from BIOSENSORS. Patrick W. Serruys reports consulting fees from SMT, Meril Life, Novartis, and Philips. The other authors declare no conflicts of interest.

Data Availability Statement

The authors have nothing to report.

References

- 1. A. Gurav, P. C. Revaiah, T. Y. Tsai, et al., "Coronary Angiography: A Review of the State of the Art and the Evolution of Angiography in Cardio Therapeutics," *Frontiers in Cardiovascular Medicine* 11 (2024): 1468888.
- 2. D. Keane, J. Haase, C. J. Slager, et al., "Comparative Validation of Quantitative Coronary Angiography Systems. Results and Implications From a Multicenter Study Using a Standardized Approach," *Circulation* 91 (1995): 2174–2183.
- 3. K. L. Gould, "Does Coronary Flow Trump Coronary Anatomy?," *JACC: Cardiovascular Imaging* 2 (2009): 1009–1023.
- 4. P. A. L. Tonino, B. De Bruyne, N. H. J. Pijls, et al., "Fractional Flow Reserve Versus Angiography for Guiding Percutaneous Coronary Intervention," *New England Journal of Medicine* 360 (2009): 213–224.
- 5. S. S. Virani, L. K. Newby, S. V. Arnold, et al., "2023 AHA/ACC/ACCP/ASPC/NLA/PCNA Guideline for the Management of Patients With Chronic Coronary Disease: A Report of the American Heart Association/American College of Cardiology Joint Committee on Clinical Practice Guidelines," *Circulation* 148 (2023): e9–e119.
- 6. C. Vrints, F. Andreotti, K. C. Koskinas, et al., "2024 ESC Guidelines for the Management of Chronic Coronary Syndromes," *European Heart Journal* 45 (2024): 3415–3537.
- 7. B. Xu, S. Tu, L. Song, et al., "Angiographic Quantitative Flow Ratio-Guided Coronary Intervention (FAVOR III China): A Multicentre, Randomised, Sham-Controlled Trial," *Lancet* 398 (2021): 2149–2159.
- 8. L. Song, B. Xu, S. Tu, et al., "2-Year Outcomes of Angiographic Quantitative Flow Ratio-Guided Coronary Interventions," *Journal of the American College of Cardiology* 80 (2022): 2089–2101.
- 9. B. K. Andersen, M. Sejr-Hansen, L. Maillard, et al., "Quantitative Flow Ratio Versus Fractional Flow Reserve for Coronary

- Revascularisation Guidance (FAVOR III Europe): A Multicentre, Randomised, Non-Inferiority Trial," *Lancet* 404 (2024): 1835–1846.
- 10. B. K. Andersen, N. R. Holm, L. J. H. Mogensen, et al., "Coronary Revascularisation Deferral Based on Quantitative Flow Ratio or Fractional Flow Reserve: A Post Hoc Analysis of the FAVOR III Europe Trial," *EuroIntervention* 21 (2025): e161–e170.
- 11. R. L. Kirkeeide, K. L. Gould, and L. Parsel, "Assessment of Coronary Stenoses by Myocardial Perfusion Imaging During Pharmacologic Coronary Vasodilation. VII. Validation of Coronary Flow Reserve as a Single Integrated Functional Measure of Stenosis Severity Reflecting All Its Geometric Dimensions," *Journal of the American College of Cardiology* 7 (1986): 103–113.
- 12. C. Girasis, J. C. H. Schuurbiers, Y. Onuma, P. W. Serruys, and J. J. Wentzel, "Novel Bifurcation Phantoms for Validation of Quantitative Coronary Angiography Algorithms," *Catheterization and Cardiovascular Interventions* 77 (2011): 790–797.
- 13. C. Girasis, J. C. H. Schuurbiers, Y. Onuma, et al., "Two-Dimensional Quantitative Coronary Angiographic Models for Bifurcation Segmental Analysis: In Vitro Validation of CAAS Against Precision Manufactured Plexiglas Phantoms," *Catheterization and Cardiovascular Interventions* 77 (2011): 830–839.
- 14. K. Ninomiya, P. W. Serruys, N. Kotoku, et al., "Anonymous Comparison of Various Angiography-Derived Fractional Flow Reserve Software With Pressure-Derived Physiological Assessment," *JACC: Cardiovascular Interventions* 16 (2023): 1778–1790.
- 15. H. Hara, P. W. Serruys, N. O'Leary, et al., "Angiography-Derived Physiology Guidance vs Usual Care in an All-Comers PCI Population Treated With the Healing-Targeted Supreme Stent and Ticagrelor Monotherapy: PIONEER IV Trial Design," *American Heart Journal* 246 (2022): 32–43.
- 16. A. Scoccia, R. A. Byrne, A. P. Banning, et al., "Fractional Flow Reserve or 3D-Quantitative-Coronary-Angiography Based Vessel-FFR Guided Revascularization. Rationale and Study Design of the Prospective Randomized Fast III Trial," *American Heart Journal* 260 (2023): 1–8.

Supporting Information

Additional supporting information can be found online in the Supporting Information section.